Adaptive Constellation Multiple Access for Beyond 5G Wireless Systems

Indu L. Shakya, and Falah H. Ali, *Senior Member, IEEE*

***Abstract*—We propose a novel non-orthogonal multiple access (NOMA) scheme referred as adaptive constellation multiple access (ACMA) which addresses key limitations of existing NOMA schemes for beyond 5G wireless systems. Unlike the latter, that are often constrained in choices of allocation of power, modulations and phases to allow enough separation of clusters from users' combined signals; ACMA is power, modulation and phase agnostic—forming unified constellations instead—where distances of all possible neighbouring points are optimized. It includes an algorithm at basestation (BS) calculating phase offsets for users' signals such that, when combined, it gives best minimum Euclidean distance of points from all possibilities. The BS adaptively changes the phase offsets whenever system parameters change. We also propose an enhanced receiver using a modified maximum likelihood (MML) method that dynamically exploits information from the BS to blindly estimate correct phase offsets and exploit them to enhance data rate and error performances. Superiority of this scheme—which may also be referred to as AC-NOMA—is verified through extensive analyses and simulations.**

***Index Terms*—NOMA, high capacity, interference mitigation, adaptive modulation, joint detection**

I. Introduction

NOMA is a promising method to share bandwidth among multiple users without subdivision in time or frequency resources [1]- [12]. Power-domain (PD)-NOMA is a well-known variant that relies on channel gain disparity of users and successive interference cancellation (SIC) method to separate co-channel users' data to give higher sum rates than orthogonal multiple access (OMA) like OFDMA [1], [2]. The SIC method used in PD-NOMA can be sensitive to co-channel users' signal power ratios [10]. When the ratios are not optimized, it is unable to decode the interference and ends up with error floor [1]. Also general assumptions in the NOMA literatures like high channel gain disparity of users may not be applicable in many practical wireless environments. As such, conventional NOMA is not yet proven to provide sustained communication to be included as work items of 3GPP standards [2].

The use of transmit signal phase rotation for NOMA to help improve detection using SIC and other methods is adopted in [3]- [8]. The scheme in [6] proposes to use phase rotation as a mean to increase time diversity gain assuming block fading of underlying channels while using single-user receivers. It is known that the SIC outperforms single-user receivers when users' channel gains are disparate. The work [3], [7] [8] use phase rotation optimization while using SIC. However, SIC method treats other users' signals as noise. So, their gains are limited when users have similar channel gains. The phase rotation-based schemes addressing limitations of SIC with joint detection (JD)—also referred to here as JD-NOMA—are proposed in [4], [5], [9]. But they are limited to two users with [QPSK, QPSK] or [QPSK, 16-QAM] setups and limited power allocation ratios of users due to strict rules to cluster constellation points within the boundary of I/Q axes. If higher rotations are imposed, the receivers cannot easily separate data as their detection boundaries become very complicated.

We solve issues of NOMA schemes using a power, modulation and phase agnostic ACMA; where both transmission and detection systems work together to minimize probability of error for users. We devise a novel algorithm at the BS that forms unified composite signals designed to maximize the distance of each neighbour points rather than clusters. Here users' signal phases are blind adaptively rotated up to the full potentials utilizing already available knowledge of powers and modulations. Unlike JD-NOMA, it is not limited to small set of power and modulation choices only, making it suitable for diverse channel gain conditions. We also propose an effective MML based receiver to capitalize on the synergy provided by the BS and parameters it shared via control channels to blindly find and apply correct phase offsets to give best possible data rate and error performances. We prove superiority of ACMA through extensive analyses and simulation results.

II. Signal and System Models

We consider a downlink system with K users served simultaenously by a base-station. The constituent modulated symbol of each user x_k is taken from a square M-QAM constellation with symmetric in-phase (I) i_k and quadrature (Q) q_k components as follows: $x_k = i_k + \sqrt{-1}q_k$. Note that the ACMA approach is about intelligent use of constellation information and as such, it is generic enough to be used for both uplink and downlink using diverse modulation methods like M-QAM, M-PSK. Each user's symbols have alphabet of size M_k. The symbols are then multiplied by modulation specific scaling factor to ensure unity expected energy $\mathbb{E}\{|x|^2\} = 1$. The BS then applies user specific power allocation coefficients α_k to suit power budget for various conditions. This is also done to ensure that the ACMA composite signals maintain the same average and peak power constraints as in single-user case for fair reference i.e. $P_T = \sum_{k=1}^{K} P_k; P_k = \alpha_k P_T$. The composite

Manuscript received xxxxxxxxxxx y, 2023; revised xxxxxx y, 2023. The editor coordinating the review of this letter was xxxxxxxxxxxxxxxxx. (Corresponding author: Indu L. Shakya.)

Dr Indu L. Shakya is a technology leader and consultant for wireless and satellite communications industries (ishakya@gmail.com). He is also a research collaborator with the University of Sussex, UK. Falah H. Ali is a professor of Communications Engineering at the School of Engineering and Informatics, University of Sussex, Brighton, BN1 9RH, UK. (F.H.Ali@sussex.ac.uk).

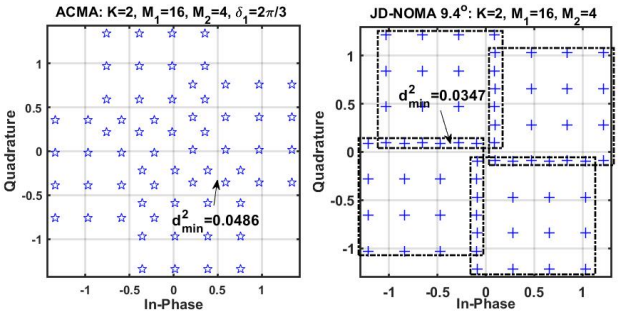

Fig. 1: Constellation of a) proposed ACMA and b) JD-NOMA [4], [5] clusters for a two-user system using 16-QAM and 4-QAM and power allocation factors of $[\alpha_1, \alpha_2] = [0.35, 0.65]$. Phase offsets of $\delta_1 = 2\pi/3$ by the former and 9.4° by the latter are generated, leading to different d^2_{min}.

constellation of K users s, transmitted from the BS can be written as:

$$s = \sum_{k=1}^{K} \sqrt{\alpha_k P_T} x_k \exp(j\theta_k + \delta_k), \quad (1)$$

where $\theta^k = \angle(x_k)$ is an initial phase angle of a user's original M-QAM signals and δ_k is a user specific phase offset coefficient. We use a baseband model of users' radio propagation channels to elucidate key differences of interference mitigation mechanisms of different NOMA transceiver algorithms. We assume all schemes apply the same approach to compensate for the large and small scale path losses to aid the detection of user' data by adjusting the parameters $\alpha_k, k = 1, 2, .., K$ where $0 \leq \alpha_k P_T \leq P_T, \forall k$. The signal at the receiver of user k can be written as:$r_k = h_k s + z_k; k = 1, 2, .., K$, where h_k represents baseband model of complex fading channel between the BS and user k. We also assume independent Rayleigh distribution for fading channels with $\mathcal{CN}(0, 1)$. Finally, z_k represents the additive white Gaussian noise (AWGN) component with $\mathcal{CN}(0, N_0)$.

III. Proposed Transceiver Designs

A. Conventional PD-NOMA Transceivers

In relation to (1) a PD-NOMA e.g. [1] can be seen as a special case by setting $\delta_k = 0, \forall k$, i.e. the BS does not adapt transmitted signal constellations. It uses SIC receiver which works on the assumption that users that are closer to the BS achieve higher SNR compared to users that are further away to form easily discernible clusters. Hence a receiver for a near user l can readily decode the data sent to far users $l+1, .., K$, then use the estimated data $\hat{x}_{l+1}, .., \hat{x}_K$ to regenerate their interference and subtract the sum from the total received signal r_l, to form a more reliable estimate $\hat{x}_l$ as:

$$\hat{x}_l = \arg \min_{x_l \in \mathbb{X}_l} \left| r_l - \sum_{k=l+1}^{K} \hat{h}_l \sqrt{\alpha_k P_t} \hat{x}_k - \hat{h}_l \sqrt{\alpha_l P_t} x_l \right|^2, \quad (2)$$

where, $\mathbb{X}_l = [x_1, x_2, .., x_{M_l}]^T$. SIC work satisfactorily when proper power ratio is used such that $\alpha_{l+1}/\alpha_l >> 1$ [11], [12]. The ratio, if unoptimized can lead to inevitable error floors even if SNR increases monotonically [1], [4]. Although the entropy maximizing phase rotation method of [7] show small gain over PD-NOMA with SIC, it too can not resolve error floor trends when power ratio is not satisfied.

TABLE I: ACMA Algorithm for Calculating Phase Offsets

1) Obtain input parameters: $K, M_k, P_T, \alpha_k; k = 1, 2, .., K$.
2) Set all possible phase offset matrix for all users of size $K \times V$ to 0, $\delta = [\mathbf{0}]_{K \times V}$.
3) Initialize a vector of all d^2_{min} values for all users, $\mathbf{d}^2_{min(k)} = [\mathbf{0}]_{K \times V}$.
4) for $k = 1 : K$
5) if $k = K$
6) $\delta_k = \delta_{k,v}$
7) else
8) for $v_k = 1 : V$
9) a) For each v, calculate $d^2_{\min}$ using (4);
10) b) Update $\delta_{k,v} = \frac{2\pi}{V - v + 1}$;
11) end
12) Pick the $\delta^{k,v}$ that gives maximum d^2_{min};
13) Update final $\delta_k = \delta_{k,v}$;
14) end.
15) end.
16) Return $\delta = [\delta_1, \delta_2, .., \delta_K]$.

B. JD-NOMA Transceivers with Phase Rotation

The JD-NOMA [4], [5] can address some limitations of PD-NOMA with SIC. But their operational power ranges and phase rotations are dictated by separate equations specific for each modulation and power setups to restrict points to I/Q axes to form discernible clusters. Their receivers extract data $\hat{x}_k$ by comparing r_k against composite signals of all possible transmitted data combinations $\mathbb{X}_k, k = 1, 2, .., K$ as follows:

$$\hat{x}_k = \arg \min_{x_1 \in \mathbb{X}_1, .. x_K \in \mathbb{X}_K} \left| r_k - \hat{h}_k \sum_{k=1}^{K} \sqrt{\alpha_k P_t} x_k \right|^2. \quad (3)$$

As (3) cannot resolve detection ambiguity when points cross I/Q axes, phase rotations applied for JD-NOMA are limited to small values. This leads to lower d^2_{min} as shown in Figure 1.

C. Proposed ACMA Transceivers

Continuing with the Figure 1, we can see that phase rotation optimization of the ACMA is not limited to be within the I/Q boundaries i.e. points are allowed to cross over. Moreover they are not limited to $K = 2$ and certain modulations only $[M_1, M_2] \in [4, 4], [16, 4]$ as in [4], [5]. With ACMA the BS transmits composite data s which uses constellation points by adjusting each user's signal by a phase offset value δ_k given by an algorithm that autonomously adapts it to system parameter changes K, $\alpha_k, M_k, k = 1, 2, .., K$ until the best d^2_{min} found. The spread of constellation points becomes progressively denser with increase in $k = 1, 2, .., K$. But each iteration is independent, adding complexity only linearly. The algorithm is detailed in Table I.

Here $d^2_{\min}$ is selected from all possible $d^2_{a,b}$ that are the distances of a transmitted ACMA signal from all possible K

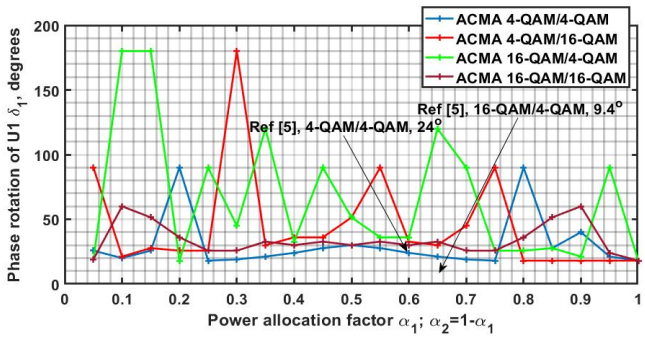

Fig. 2: Phase rotation δ_1 of user U1 for ACMA for $K = 2$, different M_1-QAM/M_2-QAM configurations, $V = 20, Q = 20$ under different power sharing values of α_1 and α_2. Rotation values from JD-NOMA [5] are also included for reference.

users' data combinations of size $\prod_k^K M_k$ against all other $\prod_k^M M_k - 1$ signal possibilities as given in (4). The $d^2_{\min}$ values are then calculated for V phase offset values $\delta_{k,v}, v = 1, 2, .., V$ covering the full 2π radians and the one that gives highest $d^2_{\min}$ is updated to give δ_k. Note that full set of $\delta_k, k = 1, 2, .., K$ values for all configurations $P_T, M_k, \alpha_k, \forall k$ $Q = P_T/\min(\alpha_k - \alpha_l), k \neq l$, can be calculated offline and stored in memory as lookup tables, its use does not add latency. We show a plot of these values in Figure 2 for $M_k \in \{4, 16\}, \forall k$, under the full range of $[\alpha_1, \alpha_2]$. The complete ACMA transceiver algorithm is given Table II.

The system can also be configured to operate in both static and dynamic user environments. For the former, the BS sets $\phi_k, k = 1, 2, .., K$ only once after all receivers have been calibrated. For the latter, the BS adjusts paramaters including $\delta_k, k = 1, 2, .., K$ upon the signal quality feedback from receivers. The BS shares info $K, P_T, M_k, \alpha_k, k = 1, 2, .., K$ to receivers. This may be done via downlink control information (DCI) slots of PDCCH of LTE, 5G NR standards. Signalling overheads for this are expected be small.

The receiver estimates transmitted data by using the MML joint detection method given in (5), which compares r_k against the reconstructed signal of all likely data $x_k \in \mathbb{X}_K, k = 1, 2, .., K$, $\hat{\delta}_k$ and shared parameters $P_T, K, \alpha_k, M_k, k = 1, 2, .., K$. It also estimates all possible $\hat{\delta}$ independently using the algorithm in Table I and store in memory. The process in (5) uses a simple lookup process for picking phases $\hat{\delta}_k, k = 1, 2, .., K$ which does not introduce extra latency.

D. Comparison of Computational Efforts

In Table III we compare computational efforts of ACMA transceivers against PD-NOMA, JD-NOMA. We simplify expressions using an average of users' modulation alphabets $\mu = \sum_{k=1}^K M_k/K$. PD-NOMA requires lower computational efforts than ACMA and JD-NOMA. This is mainly due the latter using joint detection of all K users signals at the receiver side scaling at the rate of μ^K searches. ACMA requires some additional offline pre-processing that needs V phase offset searches against Q possible power steps per user to arrive at the d^2_{min} optimized constellations, totalling $KQV(\mu K)^2$ multiplications. It should be noted that number of co-channel users K for any NOMA access is essentially small e.g. 2, 3 in practice which makes computational demand less of an issue for online ACMA data detection algorithms.

TABLE II: The ACMA Transceiver Algorithm Steps

Basestation Transmitter
1) Obtain input parameters:
P_T, M_k, α_k, $\Psi, \phi^k, k = 1, 2, .., K$.
2) Map each user's data bits into a M-QAM/M-PSK signal x_k.
if $\Psi = 0$
Dynamic users' environment
3) Update $\theta^k = \angle(x_k), \forall k$.
4) Calculate $\delta^k, k = 1, 2, .., K$ using the algorithm in Table I.
else
Static users' environment
5) Set $\theta^k = \angle(x_k)$; $\delta_k = \phi^k, k = 1, 2, .., K$.
end
6) Form composite ACMA signal as per (1).
7) Share P_T, K, V, Q $\alpha_k, M_k \forall k$ to users via control channels.
8) Transmit signal s.
Receiver k^{th} user
1) Decode the shared data P_T, K, V, Q $\alpha_k, M_k, \forall k$.
2) Calculate $\hat{\delta}$ using algorithm in Table I and store as lookup.
3) Initialize users' likely transmitted signals $\hat{\mathbf{x}} = [0, 0, .., 0]_{K\times 1}$.
4) Obtain $\hat{\delta}_k, \forall k$ for each $\alpha_k, M_k \forall k$ update using the lookup table.
5) Update $\hat{\mathbf{x}}$ using the MML detection method in (5).
6) Extract desired data $\hat{x}_k \in \hat{\mathbf{x}}$.
7) Report estimates of received power from r_k to BS periodically.

TABLE III: Computational Efforts Of ACMA Transceivers Against PD-NOMA and JD-NOMA

Scheme	Multiply	(Add)/(Subtract)	Offline Process
PD-NOMA [1]	$K\mu + K\mu$	$(K/2)/(K^2/2)$	–
JD-NOMA [4], [5]	$K\mu + \mu^K$	$(K)/(K)$	$K^2Q\mu\log(V)$
ACMA	$K\mu + \mu^K$	$(2K)/(K)$	$KQV(\mu K)^2$

IV. Numerical Results and Discussions

Here we use simulation results to compare symbol error rate (SER) and throughput of ACMA against the other schemes. Two-user system $K = 2$ used for clarity and ease of comparisons, with M-QAM signals $M_k \in \{4, 16\}$ and vary $\alpha_1 \in [0{-}1]$ where $\alpha_2 = 1{-}\alpha_1$ for all schemes. Systems using $K > 2$ add extra computational efforts, but the performace trends of all schemes are expected to continue. For ACMA $Q = 20, V = 20$ and $\Psi = 0$ assumed. Estimation of channel and other parameters is assumed perfect $\hat{h}_k = h_k, \hat{\delta}_k = \delta_k, \forall k$. In practice carrier frequency, channel and phase are estimated using phase locked loop and reference symbols. Estimation error impact SER and specially when M_k is high [14].

In Figure 3 a) and b), we present SER of ACMA for $K = 2$ and $M_1 = 16, M_2 = 4$ under the same total SNR, P_t/N_0 and how they compare against other NOMA schemes under different $[\alpha_1, \alpha_2]$ values of $[0.1, 0.9]$ and $[0.35, 0.65]$, respectively. The users are labeled as U1 and U2. The SER curves for all schemes are identical for $[\alpha_1, \alpha_2] = [0.1, 0.9]$. This is expected because under controlled power allocation the SIC method in (2) is able to successfully decode the signal of U1, subtract its interference to U2 to obtain cleaner signal giving the same results as the joint detection method

$$d^2_{\min} = \min\left\{d^2_{a,b}\right\} = \arg\min_{\delta_{k,v}\in\delta}\left|\sum_{k=1}^{K}\sqrt{\alpha_k P_T}x_k^{(a)}\exp(j\theta_k+\delta_{k,v}) - \sum_{k=1}^{K}\sqrt{\alpha_k P_T}x_k^{(b)}\exp(j\theta_k+\delta_{k,v})\right|^2, \forall a\neq b. \quad (4)$$

$$\hat{\mathbf{x}} = \arg\min_{x_1\in\mathbb{X}_1,..x_K\in\mathbb{X}_K\hat{\delta}_1\in\delta,\hat{\delta}_2\in\delta,..,\hat{\delta}_K\in\delta}\left|r_k - \hat{h}_k\sum_{k=1}^{K}\sqrt{\alpha_k P_T}x_k\exp\left(j\theta_k+\hat{\delta}_k\right)\right|^2. \quad (5)$$

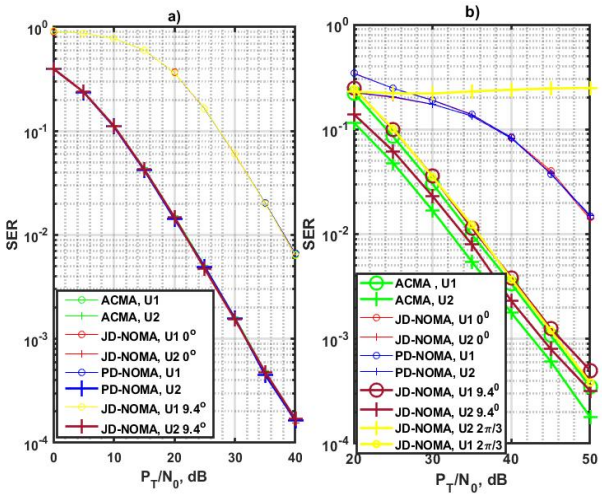

Fig. 3: SER of users U1 and U2 for ACMA compared with JD-NOMA, PD-NOMA for $K=2$, $|h_1|^2/|h_2|^2 = 0$ dB, $M_1 = 16$, $M_2 = 4$ and for $[\alpha_1,\alpha_2]$ = a) $[0.1, 0.9]$, b) $[0.35, 0.65]$.

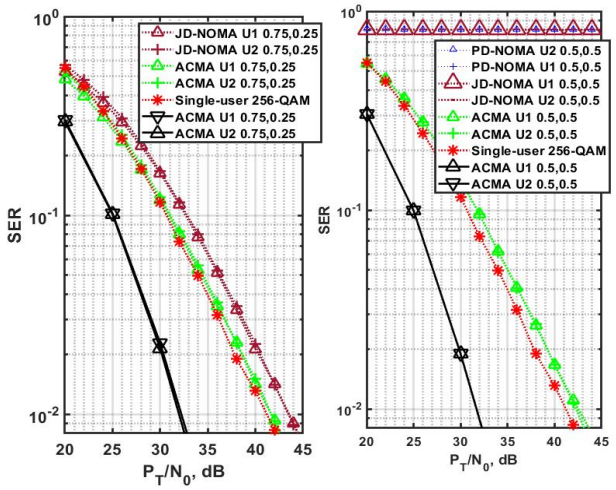

Fig. 4: SER of U1 and U2 for ACMA compared with JD-NOMA, PD-NOMA for $K=2$, $M_1=16$, $M_2=16$, $|h_1|^2/|h_2|^2 = 0$ dB, $[\alpha_1,\alpha_2]$ = a) $[0.75, 0.25]$ and b) $[0.5, 0.5]$. Two-antenna receive diversity (Solid lines).

[11]- [12]. It is worth noting that the SER of ACMA depends on how closely spaced all the possible composite signals of users' are relative to each other regardless of which quadrant the constellation points are located i.e. d^2_{min} in (4). For $[\alpha_1,\alpha_2] = [0.35, 0.65]$ ACMA offers better SER compared with others. It outperforms JD-NOMA even with its optimal rotation of $9.4°$ by $\approx$ 2 dB at the SER of 10^{-2}. This is because it achieves greater d^2_{min} by adapting phase offset of U1 to reach highest d^2_{min} with $\delta_1 = 2\pi/3$. PD-NOMA and JD-NOMA without phase rotation ($0°$) lag ACMA by >15 dB due to increase in unresolved magnitude and phase noise. For completeness we also plot SER of JD-NOMA with rotation of $2\pi/3$ to U1 signal. As can be seen from Figure 3 b), while U2 performs close to ACMA, U1 suffers error floor as the JD-NOMA receiver has no way to resolve it by identifying the detection boundaries from the composite signals.

In Figure 4 a) and b), we show SER with $M_1 = 16, M_2 = 16$ for different $[\alpha_1,\alpha_2]$ of $[0.75, 0.25]$ and $[0.5, 0.5]$, respectively. Under higher order M_k, constellation points become closer with much higher probabilities of them crossing the boundaries of users' modulated signals. The JD-NOMA schemes in [4], [5] do not provide phase rotation parameters for $M_1 = 16, M_2 = 16$. Looking at Figure 1 we expect phase rotation to deminish $\to 0$. ACMA achieves ≈ 2 dB gain over JD-NOMA at the SER of 10^{-2} for $[\alpha_1,\alpha_2 = [0.75, 0.25]$ as it finds better d^2_{min} by adjusting δ_1. For $[\alpha_1,\alpha_2] = [0.5, 0.5]$, JD-NOMA exhibits error floor similar to PD-NOMA, but ACMA does not. Even under such an extremely tight constellation signals, ACMA achieves SER of 10^{-2} at the cost of ≈ 2 dB over single-user 256-QAM. We also use simple analysis to estimate its SER of ACMA. As it does not treat co-channel users as noise or interference, we can use the SNR vs. SER relation of ordinary M-QAM signals of size $\Sigma = \prod_{k=1}^{K} M_k$ and adjust it by a ratio $\min\{d^2_{ACMA}\}/\min\{d^2_{\Sigma-QAM}\}$ to give its upper bound: $SER_{ACMA} \leq SER_{\Sigma-QAM}\Big\{P_T/N_0 \times \min\{d^2_{ACMA}\}/\min\{d^2_{\Sigma-QAM}\}\Big\}$. This approach predicts a max SER slope of ACMA 2.6 dB worse than that of single-user 256-QAM–which the results in Figure 4 support. It is clear that, for higher K higher SNR is required to decode users' data. Use of spatial diversity can significantly reduce the SNR required in such cases. Figure 4 shows SER gains of ≈ 10 dB with two receive antennas for both cases.

In Figure 5 we compare SER of ACMA for $M_1 = 16, M_2 = 4$, and $M_1 = 16, M_2 = 16$, while varying α_1, ($\alpha_2 = 1-\alpha_1$) until they use equal powers of 0.5 for the same P_t/N_0 dB. In the Figure 5 a), PD-NOMA shows degraded SER for $\alpha_1 > 0.1$. JD-NOMA uses optimal rotation of (16) in [5], giving improved SER compared to PD-NOMA. Both schemes fall short of SER of ACMA when powers allocated to users are similar i.e $\alpha_1 \to 0.5$. In Figure 5 b), for SER trends continue. Here we use JD-NOMA with $0°$ phase rotation for U1. ACMA continues to show better SER, specially when $\alpha_1 \to 0.5$. The resilience of ACMA can make it a very attractive choice to ease grouping of users without needing them to be at certain distance ratios from the BS [10] and to sustain data communications in extreme conditions.

Continuing for $K = 2, M_1 = 16, M_2 = 16$, in Figure 6 we compare sum data throughputs Ω of ACMA for different $[\alpha_1,\alpha_2]$ values and for two channel conditions $|h_1|^2/|h_2|^2 = [0, 20]$ dB. The $\Omega = \sum_{k=1}^{K}\log_2(M_k)[1-\text{SER}_k]$ is a useful

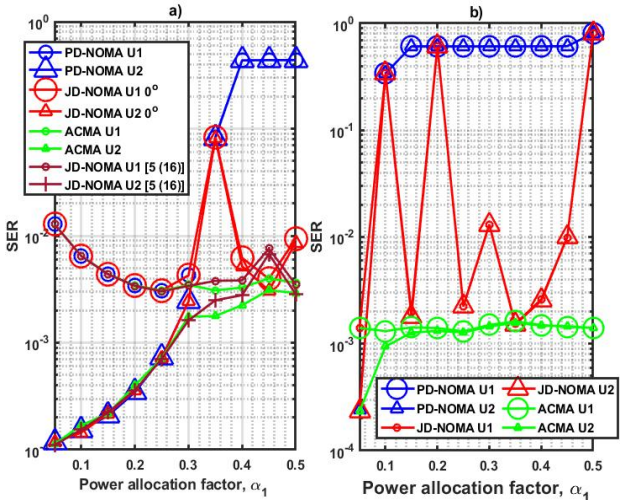

Fig. 5: SER of ACMA for U1 and U2 compared with JD-NOMA and PD-NOMA under $|h_1|^2/|h_2|^2 = 0$ dB for a) $M_1 = 16, M_2 = 4, P_t/N_0 = 40$ dB, and b) $M_1 = 16, M_2 = 16, P_t/N_0 = 50$ dB, for different α_1 values in the range $[0.05 - 0.5]$ where $\alpha_2 = 1 - \alpha_1$.

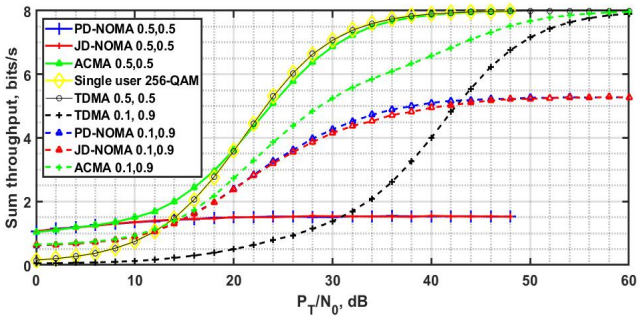

Fig. 6: Sum throughput of ACMA compared with TDMA, JD-NOMA and PD-NOMA for $K = 2$ $[M_1, M_2] = [16, 16], [\alpha_1, \alpha_2] = [0.1, 0.9]$ and $[0.5, 0.5]$. Solid lines are for $|h_1|^2/|h_2|^2 = 0$ dB and dotted lines for $|h_1|^2/|h_2|^2 = 20$ dB.

metric in comparing SER achieved to maintain a fixed data rate. We also show SER of TDMA under the same conditions where we allocate proportional power $\alpha_k P_T$ and time-slot α_k resources to users. For $[\alpha_1, \alpha_2] = [0.5, 0.5], |h_1|^2/|h_2|^2 = 0$ dB, ACMA achieves higher throughput compared with JD-NOMA and PD-NOMA. Throughputs of TDMA and single-user 256-QAM are also plotted, where ACMA shows comparable performance. For $[\alpha_1, \alpha_2] = [0.1, 0.9], |h_1|^2/|h_2|^2 = 20$ dB, ACMA achieves higher sum throughput compared with all other schemes. For example, it achieves 6.5 bits/s at the $P_T/N_0 = 40$ dB compared with ≈ 5 bits/s for PD-NOMA/JD-NOMA and 4 bits/s for TDMA. This is because ACMA balances the constellation points to give best possible detection even when they are very tightly spaced for higher M_k.

V. Conclusions

We investigated a new ACMA approach that resolves key limitations of existing NOMA transceivers in practical wireless environments where high channel gain disparity assumption of users cannot always be satisfied. We showed that the PD-NOMA and JD-NOMA can suffer from inevitable error floor if power allocation to grouped users are not set within the required ratios. Such constraints can lead to waste of power or data throughputs due to part of BS power not being utilized fully. We showed that adaptive phase offset approach of ACMA gives flexibility in power, modulation allocations and better minimum distances leading to better SER and data rates. For example, it achieves 6.5 bits/s compared with 4 for TDMA and requires ≈ 2 dB less power than JD-NOMA even with best phase rotation configurations. It shows higher gains especially when users need to be allocated similar powers, e.g. when they are within similar distances from the BS and likely in practice. Computational efforts of ACMA are reasonable for most practical cases. The use of multiple antenna transmission and reception or MIMO approach can increase the throughput and reliability of ACMA much further. Also, investigation of techniques lowering feedback overheads e.g. [13] will be interesting for future work.

References

[1] I. Lee and J. Kim, "Average Symbol Error Rate Analysis for Non-Orthogonal Multiple Access with M-Ary QAM Signals in Rayleigh Fading Channels," *IEEE Commun. Letters*, vol. 23, no. 8, pp. 1328–1331, Jun. 2019.

[2] B. Makki, K. Chitti, A. Behravan and M. -S. Alouini, "A Survey of NOMA: Current Status and Open Research Challenges," *IEEE Open J. Commun. Soc.*, vol. 1, pp. 179-189, 2020.

[3] X. Guan, Q. Yang, Y. Hong, and C. -K. Chan "Non-orthogonal multiple access with phase predistortion in visible light communication," *Optics Express*, Vol. 24, No. 22, 31 Oct 2016.

[4] X. Guan, Q. Yang and C. -K. Chan, "Joint Detection of Visible Light Communication Signals Under Non-Orthogonal Multiple Access," *IEEE Photo. Tech. Letters*, vol. 29, no. 4, pp. 377-380, 15 Feb.15, 2017.

[5] Y. Chang and K. Fukawa, 'Non-orthogonal multiple access with phase rotation employing joint MUD and SIC', *IEEE Veh. Technol. Conf.*, vol. 2018-June, pp. 1–5, 2018.

[6] M. Qiu, Y.-C. Huang, and J. Yuan, 'Downlink Non-Orthogonal Multiple Access Without SIC for Block Fading Channels: An Algebraic Rotation Approach', *IEEE Trans. Wirel. Commun.*, vol. 18, no. 8, pp. 3903–3918, 2019.

[7] N. Ye, A. Wang, X. Li, W. Liu, X. Hou, and H. Yu, 'On constellation rotation of NOMA with SIC receiver', *IEEE Commun. Lett.*, vol. 22, no. 3, pp. 514–517, 2018.

[8] C. H. Lin, S. L. Shieh, T. C. Chi, and P. N. Chen, 'Optimal inter-constellation rotation based on minimum distance criterion for uplink NOMA', *IEEE Trans. Veh. Technol.*, vol. 68, no. 1, pp. 525–539, 2019.

[9] B. K. Ng and C. T. Lam, 'Joint Power and Modulation Optimization in Two-User Non-Orthogonal Multiple Access Channels: A Minimum Error Probability Approach', *IEEE Trans. Veh. Technol.*, vol. 67, no. 11, pp. 10693–10703, 2018.

[10] Y. Zhang, J. Wang, L. Zhang, Y. Zhang, Q. Li and K. -C. Chen, "Reliable Transmission for NOMA Systems With Randomly Deployed Receivers," *IEEE Trans. on Commun.*, vol. 71, no. 2, pp. 1179-1192, Feb. 2023.

[11] T. Assaf, A. Al-Dweik, M. S. E. Moursi, H. Zeineldin and M. Al-Jarrah, "NOMA Receiver Design for Delay-Sensitive Systems," *IEEE Systems Journ.*, vol. 15, no. 4, pp. 5606-5617, Dec. 2021

[12] F. KARA and H. KAYA, "A True Power Allocation Constraint for Non-Orthogonal Multiple Access with M-QAM Signalling," *2020 IEEE Micr. Theo. and Techn. in Wireless Commun. (MTTW)*, Riga, Latvia, 2020, pp. 7-12

[13] F. Kara, H. Kaya, H. Yanikomeroglu, B. K. Ng and C. -T. Lam, "Bit-Interleaved Multiple Access: Improved Fairness, Reliability, and Latency for Massive IoT Networks," *IEEE Internet of Things Journ.*, vol. 10, no. 18, pp. 16006-16027, 15 Sept.15, 2023

[14] A. Goldsmith, *Wireless Communications*. Cambridge, U.K.: Cambridge Univ. Press, 2005.